Transverse Fault Throw Uncertainty Assessment: Latest Advances

Soazig Corbel, Guillaume Caumon

▶ **To cite this version:**

Soazig Corbel, Guillaume Caumon. Transverse Fault Throw Uncertainty Assessment: Latest Advances. Gocad Meeting, Jun 2007, Nancy, France. hal-03169361

HAL Id: hal-03169361
https://hal.univ-lorraine.fr/hal-03169361v1

Submitted on 15 Mar 2021

HAL is a multi-disciplinary open access archive for the deposit and dissemination of scientific research documents, whether they are published or not. The documents may come from teaching and research institutions in France or abroad, or from public or private research centers.

L'archive ouverte pluridisciplinaire **HAL**, est destinée au dépôt et à la diffusion de documents scientifiques de niveau recherche, publiés ou non, émanant des établissements d'enseignement et de recherche français ou étrangers, des laboratoires publics ou privés.

Transverse Fault Throw Uncertainty Assessment: Latest Advances

Soazig Corbel and Guillaume Caumon
Gocad Research Group, Nancy Université

Abstract

Characterization of fault displacement is difficult, yet consequential for understanding fault transmissibilities or enhancing quality of structural models. In this work, we propose to study the uncertainty about the transverse component of the fault throw vector, to optimize its direction.

Each fault block of a horizon is unfolded separately without taking faults into account, in order to separate the effects of unfolding and unfaulting in horizon deformations. Then, using a sequential Monte-Carlo sampling, several fault displacement models can be generated, to therefore select a set of best models of fault displacements. The proposed method perturbs the links across fault gaps on a horizon so as to make the transverse displacement variable. For each new displacement field, the horizon is restored, and deformation analysis is used to assess the likelihood of the fault displacement. The Monte-Carlo sampling technique being reputably slow, this optimization problem is solved locally for all faults, to obtain a set of possible models efficiently.

Introduction

Lot of work has been made to characterize uncertainties in structural models, most of it being aimed at the geometry of faults and horizons [Massonnat, 2000, Lecour et al., 2001, Caumon et al., 2004]. However, fault throws also belong to these uncertainties that need to be taken into account to enhance a structural model. From a reservoir perspective, fault throw indeed controls important features such as fault extension, thickness of the damage zone and shale gouge ratio; hence, uncertainties in the fault slip affects fault transmissibilities. Fault throws are also a relevant parameter for modeling of sedimentary facies and petrophysical properties, since it controls how stratigraphic transforms are computed [Mallet, 2004]. Fault slip also comes into play in balanced restoration and in geomechanical approaches to assess the properties of fractures from strain [Macé, 2005].

However, in current reservoir modeling practice, fault throws are mainly set automatically, by assuming a fixed direction like the main dipping line for instance, and the resulting direction of the throws do not necessarily correspond to the reality.

In this work we propose to perturb the fault throws of a structural model to produce one or several models sampling possible realistic fault throw configurations. The optimization will be focused on the transverse component of the fault throw, its only free degree of liberty.

1. Reminder: global uncertainty assessment methodology

Caumon and Muron [2006] proposed a method to assess uncertainties about transverse fault throw on stratigraphic horizons. This section is a summary of their technique, which is further developed and improved in this work.

1.1. Fault throw perturbation

3D structural models consist of a set of surfaces, like for instance stratigraphic surfaces, commonly named horizons, or also faults, unconformities and salt boundaries. These surfaces are linked to each other to ensure the coherence of the model.

To properly connect a set of faults to a horizon (Figure 2), each intersection horizon/fault is defined by:

- A set of borders – A horizon is limited by one or several borders. The gap created from the intersection of a fault with a horizon is also surrounded with new borders.

- A set of throw links – The throw links are defined across fault gaps, they associate pairs of borders across each fault.

- A set of corners – The corners are defined by two or more border extremities tied by throw links. There are four different types of corners, depending on the number of faults which intersect at the corner.

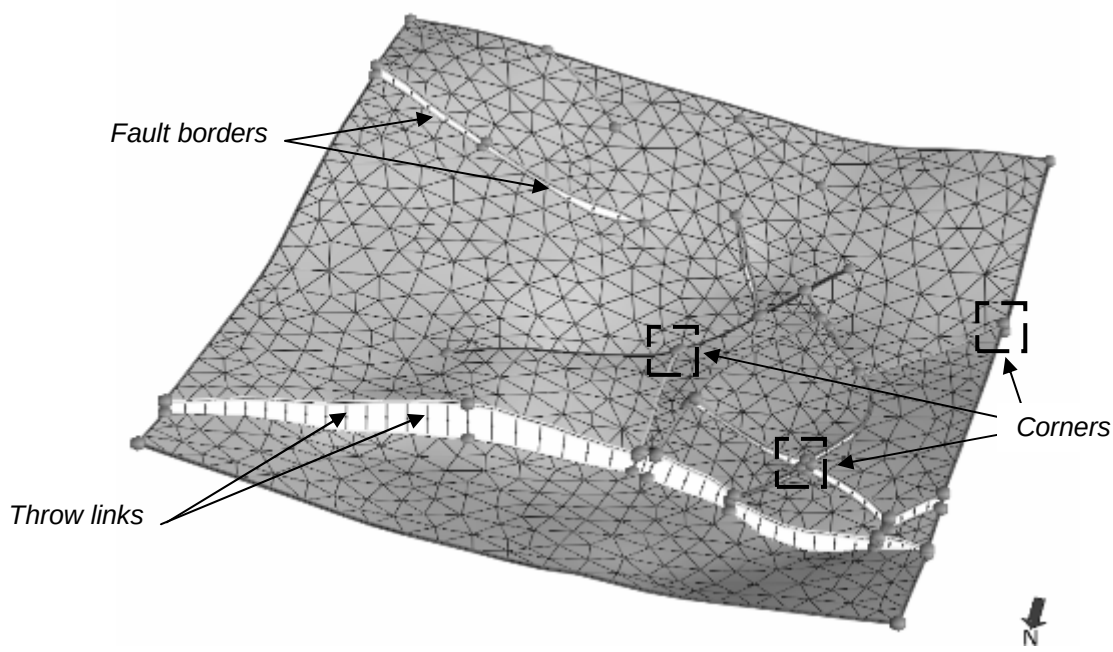

Figure 1: *Horizon coming from a structural model, courtesy of Total*
The borders of a horizon connected to a fault are colored in the same way of the corresponding fault, in order to differentiate one fault from the other ones.

As one can see, the throw links represent the throw of the faults. They are defined from one corner to another one and therefore, Caumon and Muron (2006) propose to optimize their direction by changing the geometry of the corners. For the different types of corners, the transverse throw is made variable by moving one border extremity of a corner, within its two adjacent borders (Figure 2).

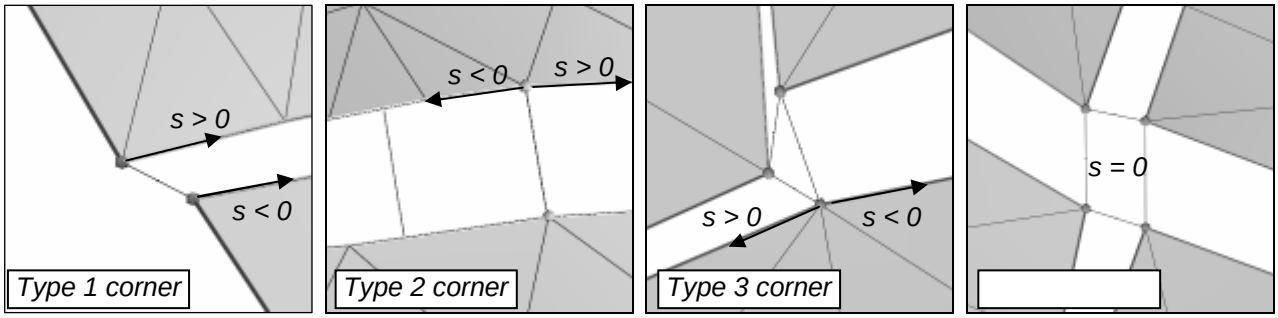

Figure 2: *Modification of the corners geometry*
Except for the fourth type of corners, all the other ones can be modified by changing the position of one border extremity. The position of this movable border extremity is defined relatively to the reference position by a curvilinear abscissa s, ranged from -1 to 1.

The perturbation assigned to the movable border extremity of a corner is randomly sampled from a cumulative probability distribution function, given in input. To modify the entire set of throw links for a global optimization, the abscissas for all corners of a given horizon are sampled one by one, using a Monte Carlo method.

1.2. Global optimization and algorithm of Monte Carlo

The sampling method used by Caumon and Muron is a Markov Chain Monte-Carlo algorithm (Figure 3).

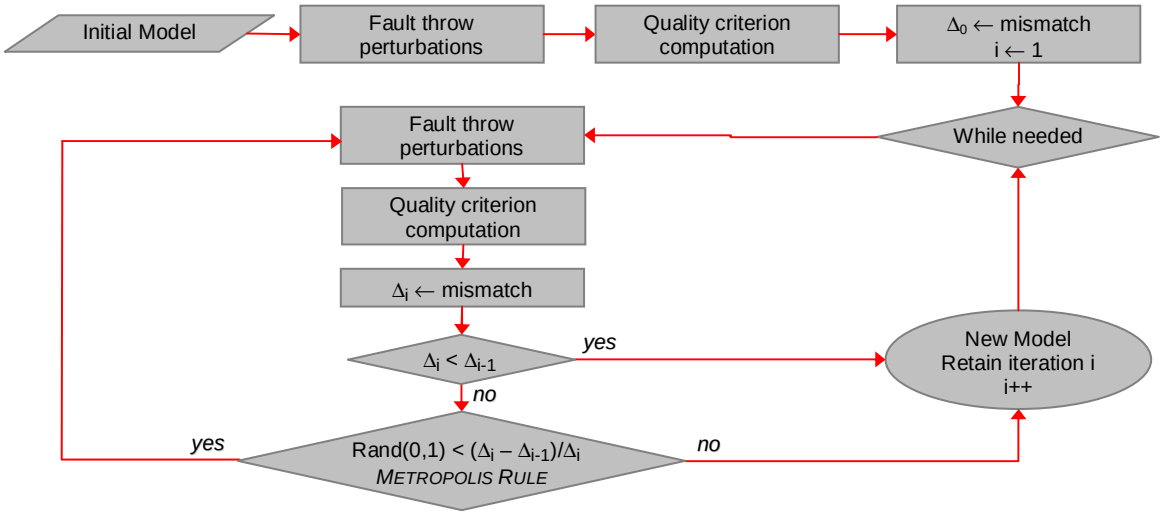

Figure 3: *Scheme of the Markov Chain Monte-Carlo algorithm*
The introduction of the Metropolis-Hastings rule enables to sample the whole fault slip posterior distribution honoring the specified likelihood criterion, and to account for possible local minima).

The algorithm is implemented so as to modify the entire set of faults at the same time, for a global optimization of the fault throws. To avoid the introduction of any bias from one realization to another one, the perturbations are set using a different random path visiting all the corners. The criterion evaluating the model quality is also computed globally, that is to say on the entire surface, using a surface restoration algorithm [Massot, 2002; Muron, 2005].

1.3. Quality criterion

To evaluate the quality of a structural model, Caumon and Muron [2006] chose to use balanced surface restoration. Basically, balanced restoration erases the consequences of both continuous and discontinuous deformations to recreate from the actual state of a geological structure, its initial state - a planar horizon.

Among the different methods available, [Gratier et al.., 1991; Rouby et al.., 1993], they performed the balanced restoration using a parameterization approach. The concept of parametric representation consists in putting into correspondence a surface S of $\mathbb{R}^3$ with a map C of $\mathbb{R}^2$, map belonging to a domain D called parametric domain (Figure 4).

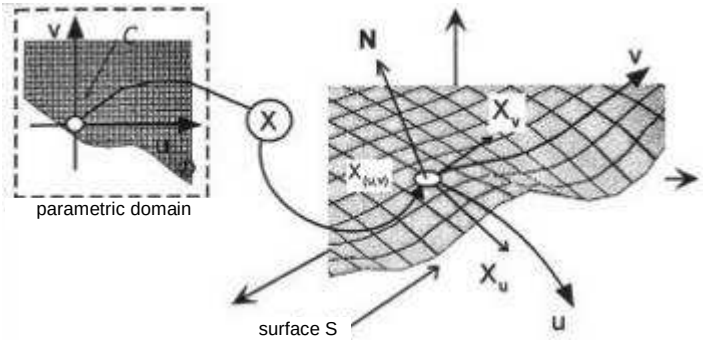

Figure 4: *Parametric representation of a surface*
There can be several parametric representations from a surface to a map. However for a given representation, a point x of S has only one image in the parametric domain (from [Massot, 2002]).

Once the balanced restoration is performed, the dilatation θ can be computed everywhere on a horizon, considering the change of area of a unit disc *dS [Mallet, 2004]*:

$$\theta = \frac{dS_{final} - dS_{initial}}{dS_{final}}$$

Three different criteria are proposed by Caumon and Muron:

1. The dilatation θ represents the first criterion capable of giving an idea of the quality of a structural model. Indeed it should be almost equal to zero, as the expanse of a horizon remains the same in spite of the deformations suffered.
2. The ratio of the principal strains λ_1/λ_2 is also a good indicator, as restoration algorithm is isotropic in nature. This criterion is a more numerical consistency check than a true physical criterion, since actual strains on a horizon may be anisotropic.
3. Eventually, the scalar product of the curvilinear frame vectors ∇u and ∇v, can also be used to evaluate the quality of a realization, as the angles should be preserved during the restoration, and therefore $\nabla u.\nabla v$ should be equal to zero.

Although the last criterion is purely mathematical the two first ones, the dilatation and the principal strains, can easily be displayed on a horizon, for a user to judge by himself of the quality of a realization (Figures 5 & 6).

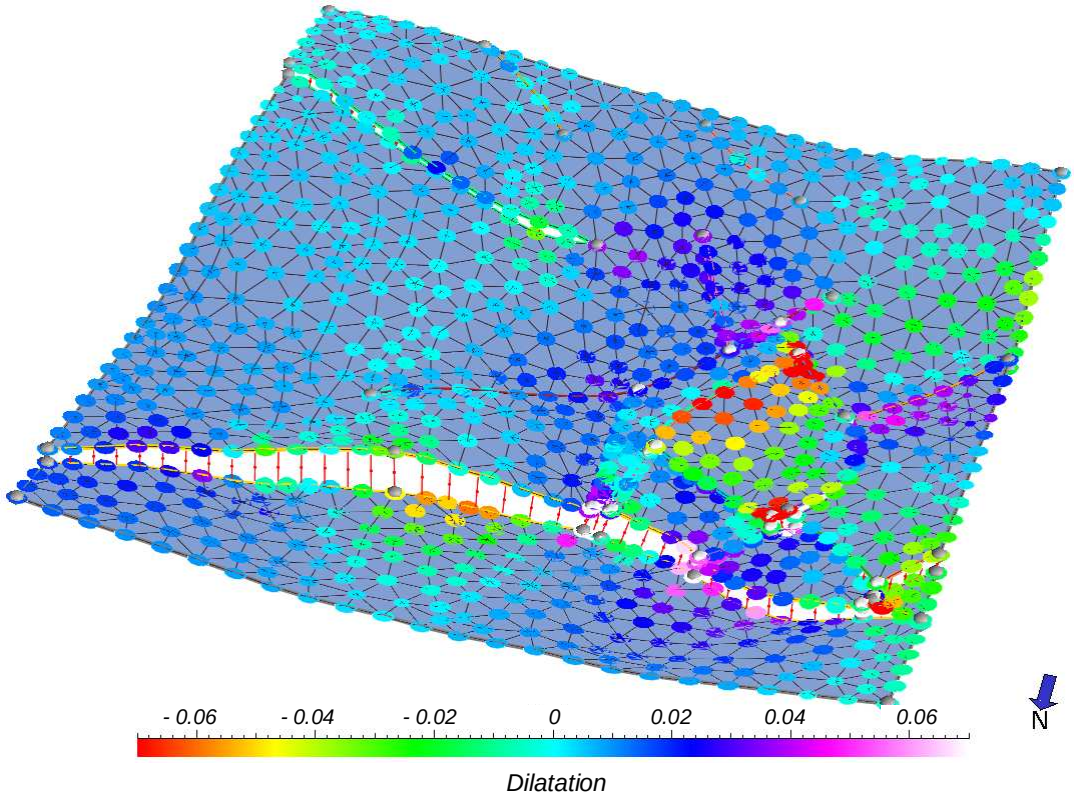

Figure 5: *Dilatation resulting from the balanced restoration of the given surface*
Whereas ellipsoids with a low dilatation degree enable to identify proper fault throws, the ones with the higher dilatation, in red or white, attest the need to modify the throws for the related faults.

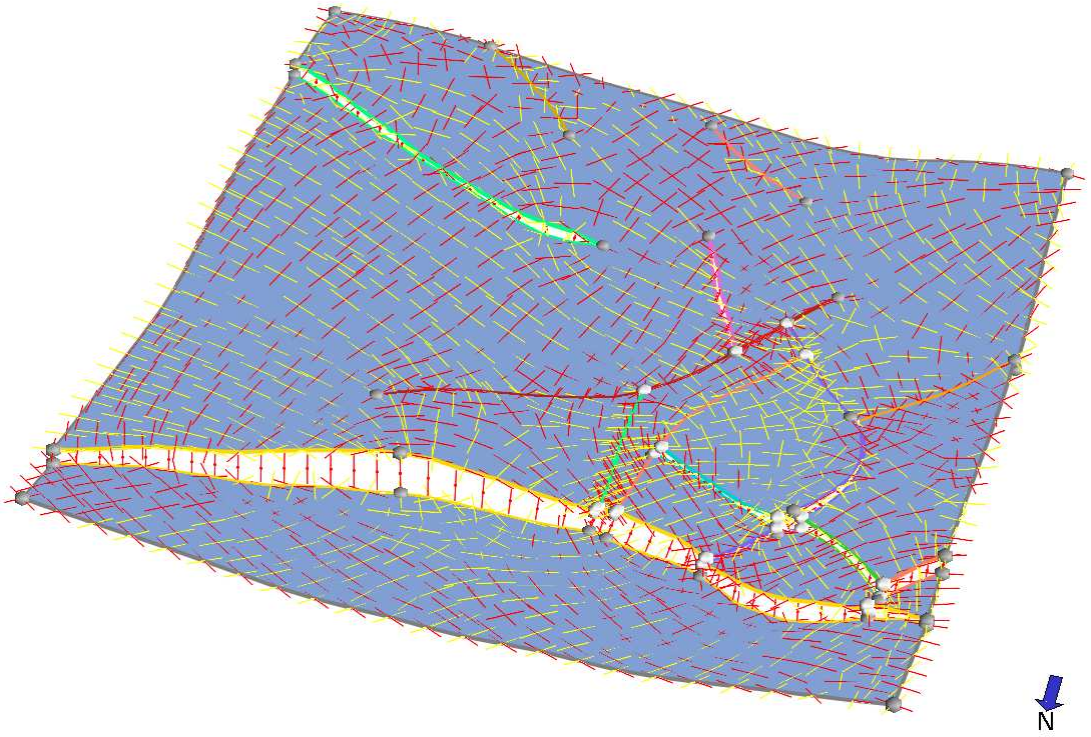

Figure 6: *Principal strain directions resulting from the balanced restoration of the given surface*
Bad fault throws can be detected by looking at the length of the principal strain vectors of strain ellipsoids, different length meaning that the throw has not been set properly. In red, strain directions are positive, in yellow they are negative.

2. Enhancement of the preexisting algorithms

To go further into the work of Caumon and Muron, a few modifications have been implemented to their algorithms. The principles of these modifications are presented below.

2.1. Local optimization of the transverse throw

In order to improve the performance of the Markov Chain Monte-Carlo algorithm, a local approach is developed. This local approach, that should correct the few imperfections existing in the global optimization algorithm, implies:

- **Optimization of fault throws one after the other**. As a global optimization modifies the geometry of all the different corners at the same time, there is no way to differentiate a throw already optimized, from a throw that still needs modifications. Therefore, the more faulted a horizon is, the less chances there are for a model to have all its fault throws optimized.
- **Computation of the quality criterion only in the neighborhood of a fault.** When the quality criterion is computed all over the horizon, it also takes into consideration the dilatation far from the faults, in areas totally independent from them. Therefore, the existence of an area with abnormally high or low dilatation can bias the sampling algorithm. Also, improvement for one fault may be hidden by a degradation for another fault, and conversely.

Let us take the example of two realizations selected from a set of 200 models (Figure 7). The criterion used to evaluate the quality of the realizations is the difference between the maximum and the minimum of the dilatation.

This local approach is has two major advantages as compared to the global criterion. First, the convergence of the sampling algorithm is better because the number of parameters is smaller. Second, the dilation spread is more focused in the neighbourhood of the fault, hence better captures improvements or degradation when the transverse slip is perturbed.

2.2. Balanced restoration performed in two steps

Another point interfering with the performance of the Markov Chain Monte-Carlo algorithm is the balanced restoration used to compute the quality criterion. When computing the quality criterion using balanced restoration from a present state of a surface to its initial state, both continuous and discontinuous deformations, respectively folds and faults, are taken into account. Yet, continuous deformations are not related to faults, there is no reason for them to be included into the quality criterion. Therefore, to avoid the interference of the continuous deformations with the quality criterion, the restoration is performed in two steps (Figure 8):

1. The first step unfolds the horizon, each fault block being restored after the other. This step does not take into account the faults and therefore erases only the continuous deformations.

2. The second step unfaults the horizon, the fault blocks being sewed to each other. The quality criterion is computed during this step, only considering the discontinuous deformations due to the movement of the fault blocks.

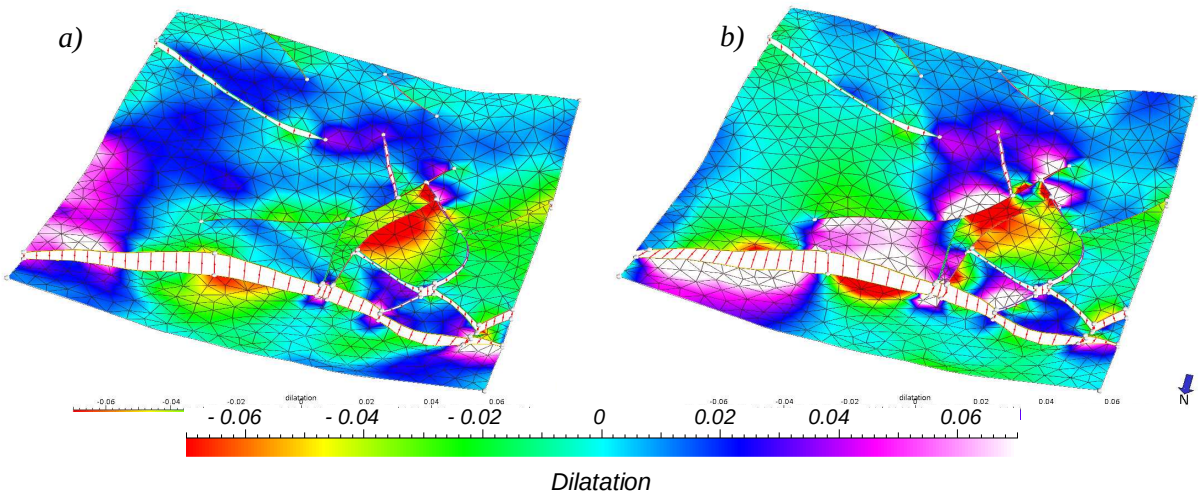

Figure 7: *Comparison between two different global optimizations*
Although the model a) has the highest criterion of 0.075, globally its dilatation is better than the one of the surface b) with a criterion of 0.035. Indeed the dilatation maximum and minimum of model b) are lower, even though still higher than 0.07 in some areas, but locally dilatation has been introduced in comparison with model a).

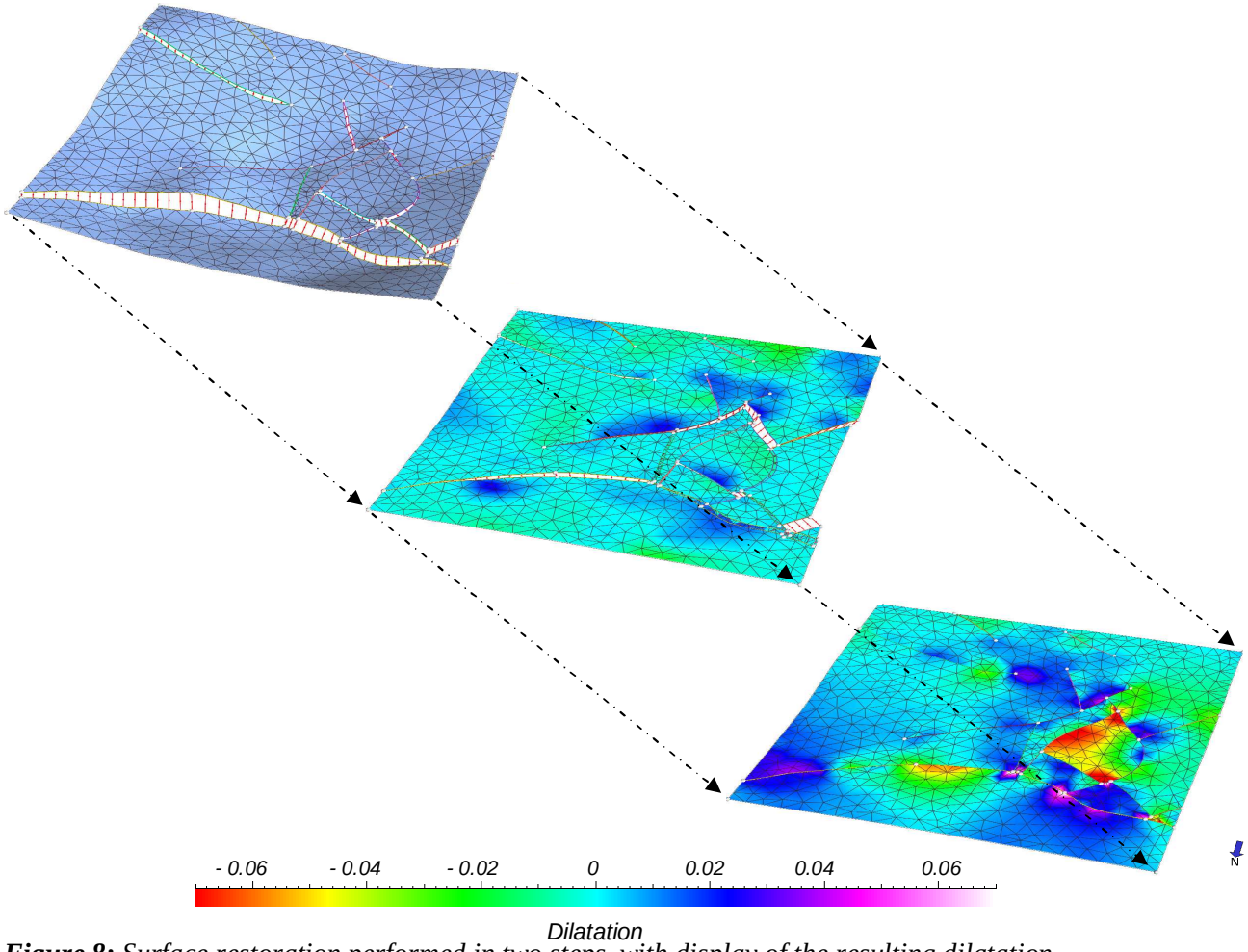

Figure 8: *Surface restoration performed in two steps, with display of the resulting dilatation*
Although the dilatations caused by the continuous deformations are lower than the ones caused by the discontinuous deformations, it can always bias the criterion in certain areas.

2.3. "Zipping" algorithm

The zipping algorithm is based on the idea that when a fault intersects a horizon, the border located on the hanging wall and the one located on the footwall should have the same length. Therefore, the "zipping" algorithm modifies the location of corners to ensure that fault borders have the same length, as far as possible. Three different types of faults need to be considered (Figure 9), as the algorithm used for each of them is slightly different.

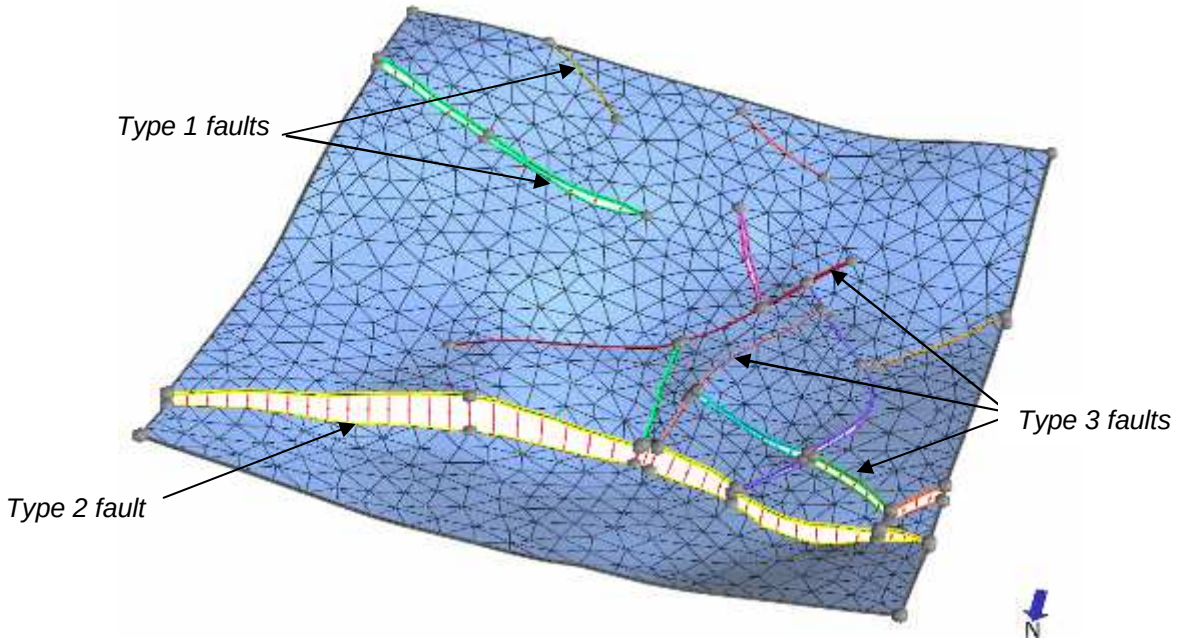

Figure 9: *Visualization of the different types of faults*

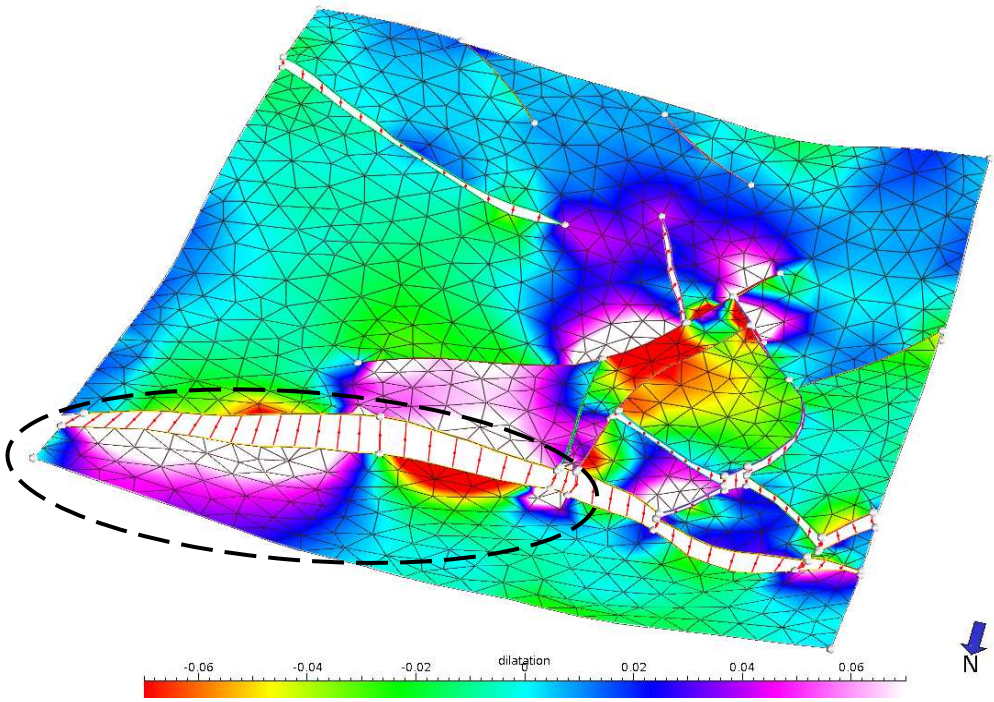

Figure 10: *Example of fault throw inconsistencies*
The major fault of the horizon is subject to high dilatation due to the way the fault throw were set.

♦ **Type 1 faults - Faults with one extremity fixed**

With only one fixed extremity, this kind of fault can be modified for the fault borders of the hanging wall and the footwall to have the same length. One after the other, the length of the borders is computed and the geometry of the corners modified in order for two associated borders to have the same length.

♦ **Type 2 faults - Faults with no extremity fixed**

With no fixed extremity, this kind of fault has no hard data to fix a reference point. The zipping algorithm works the same way than for a fault of type 1 except that the first extremity corner is modified n relation with two points of its borders, taken vertically on the hanging wall and the footwall. Then the rest of the corners are modified, for the borders of the hanging wall and footwall to have the same length.

♦ **Type 3 faults - Faults with both extremities fixed**

The both extremities being fixed, this kind of faults does not have necessarily the same global length on the hanging wall and on the footwall. Therefore, the geometry of the corners is modified for the borders to have the same curvilinear length.

The "Zipping" algorithm is performed on the surface once it has been restored a first time, in order for the continuous deformations not to bias the result. Indeed continuous deformations could modify the length of the fault borders and therefore mislead the algorithm.

2.4. Unicity of the perturbation

The global optimization approach implemented by Caumon and Muron samples one perturbation per corner. The perturbations being independent from each other, a same fault can have, on two different borders, two throws with opposite directions (Figure 10).

Although this kind of situation can happen in reality, the difference between the directions is nevertheless really low and can not go past a certain angle.

To avoid this kind of inconsistencies, only one perturbation is applied to the entire set of corners of a given fault. The perturbation is given in metric coordinates, rather than curvilinear coordinates, for the user to visualize the amplitude of the perturbation he allows.

3. Examination and critics of the results

3.1. Validation of the enhancements

Before applying the algorithms to a real dataset, let us test it on a small area of a real horizon. Without any optimization of the fault throws, the restored surface suffers some high dilatation along the faults (Figure 11).

The first step implemented to improve the fault throw uncertainty assessment is the "zipping" algorithm. To judge its efficiency, let us compare the resulting dilatation of a surface globally optimized and the one of a same surface simply "zipped" using the algorithm (Figure 12).

The dilatation is more homogeneous over the horizon and it also decreased along the faults and around the corners. However, it has to be noticed that the dilatation of certain triangles increased, which is actually coherent as the dilatation has to remain balanced.

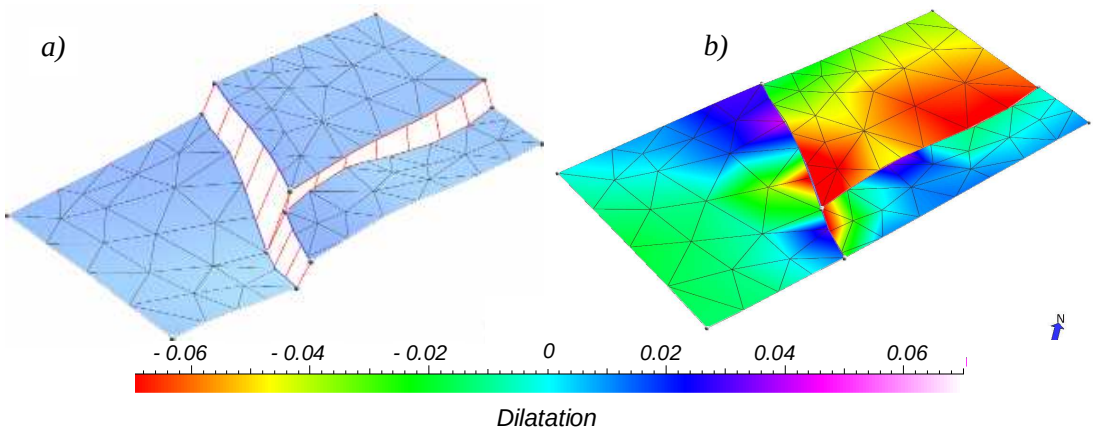

Figure 11: *Small surface and its restored state with display of the dilatation*
No fault throws were optimized before performing the restoration of surface a) and in addition, the dilatation on surface b) was computed from the discontinuous deformations.

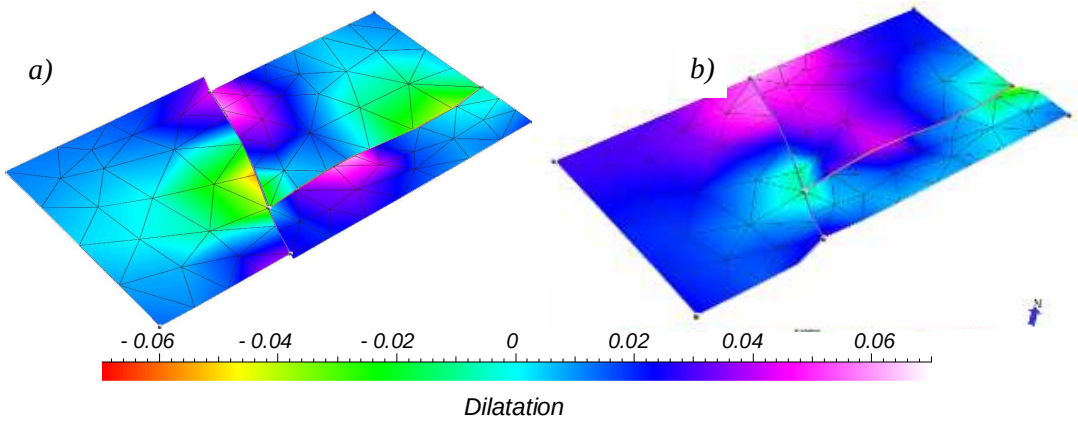

Figure 12: *a) Resulting dilatation of the surface globally optimized and restored, b) Resulting dilatation of the same surface simply "zipped" using the algorithm and then restored*

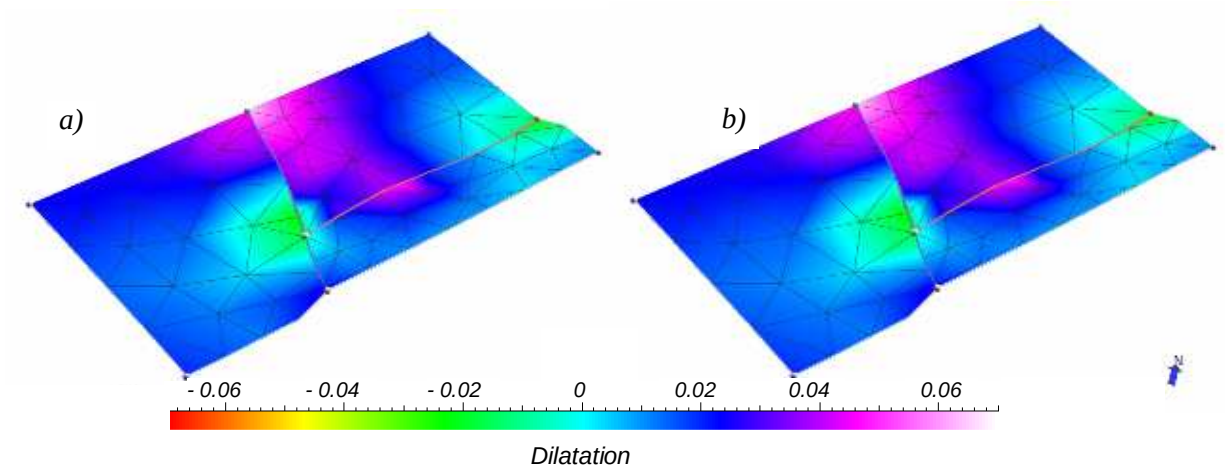

Figure 13: *Comparison between two different local optimizations*
For model a), the fault with the two extremities fixed has been optimized first, whereas for model b) it was the fault with only one extremity fixed.

Eventually, let us consider the last improvement, namely the local optimization of the fault throws. To compare the impact of the path used for the optimization, two realizations have been made, one for each possible path (Figure 13).

The two results are almost exactly the same, which is certainly due to the simplicity of the horizon. However, the influence of the path used to optimize the faults is likely really minor, even on more complex horizons. Besides, although these two models are more consistent than the model reached using the global optimization, the dilatation is not really different from the zipped model of Figure 13. Once again, these results may be due to the simplicity of the horizon.

3.2. Application to a real dataset

The surface used to properly test the new algorithms, courtesy of Total, is more complex with a set of thirteen faults. Without any optimization of the fault throws, the initial surface suffers dilatation along the faults and on the horizon borders (Figure 14).

As we did for the simple horizon, we compared one of the best models resulting of 200 simulations of global optimization and the model resulting from the "zipping" algorithm (Figure 15). Unlike the previous test, the result using global optimization is better than using only the "zipping" algorithm.

Besides, we can notice that the dilatation resulting of the zipped horizon is almost the same than the one resulting from the initial horizon. Such a small difference must be due to the fact that the corners of the initial horizon were properly set.

Eventually, the results using a local optimization instead of a global one are the following ones (Figure 16). As the dilatation was almost the same whatever the path used to optimize the fault throws, only two models are proposed here.

In comparison with the model of the global optimization, the two models obtained using the local optimization are more consistent and homogeneous. The dilatation of almost the whole horizon is ranged from -0.02 to 0.02, except for a few areas. The improvements are efficient even on a complex horizon.

Conclusion

Subsurface uncertainty modeling has long been limited to petrophysical uncertainty assessment through geostatistical stochastic modeling. However, it is clear that a significant part of subsurface uncertainty stems from the lack of structural and sedimentological informations, and also from model simplifications. Proper uncertainty assessment then relies on randomizing structures and geological scenarios.

In this paper, we have proposed improvements for algorithms implemented by Caumon and Muron. From the datasets we tested, these improvements seem to give better results and also using less realizations. However, this method currently uses one single scalar criterion to screen surfaces, mainly the dilatation. Using a combination of several restoration quality metrics would definitely improve the results obtained and be less dependent of the user, who finally currently decides which model is the best.

Acknowledgements

We would like to thank Bruno Lévy Pierre Muron and Julien Massenet for providing the surface restoration and visualization code. We would also like to thank the industrial and academic members of the Gocad Consortium for their support, and Paradigm Geophysical for providing the Gocad software and API.

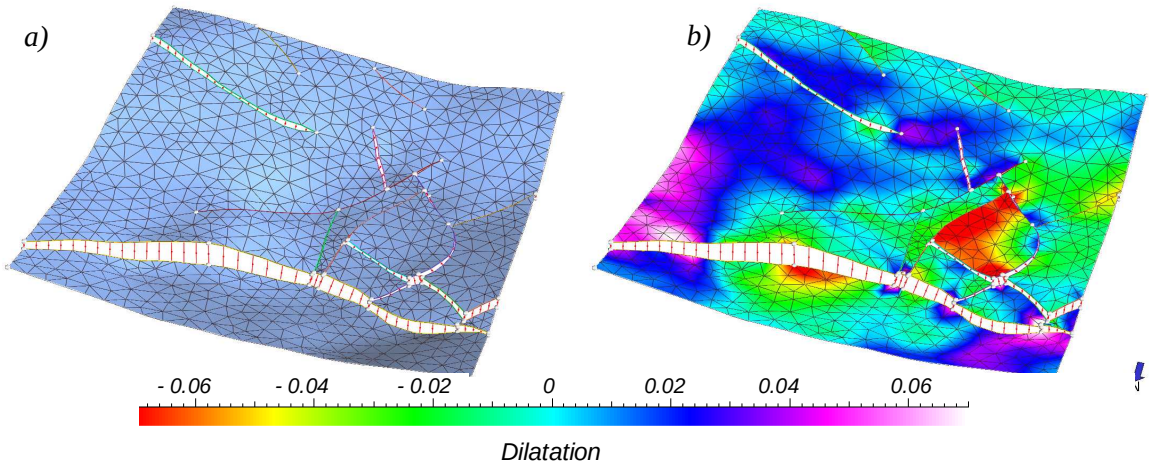

Figure 14: *Real surface and its restored state with display of the dilatation*
No fault throws were optimized before performing the restoration of surface a) and in addition, the dilatation on surface b) was computed from the discontinuous deformations.

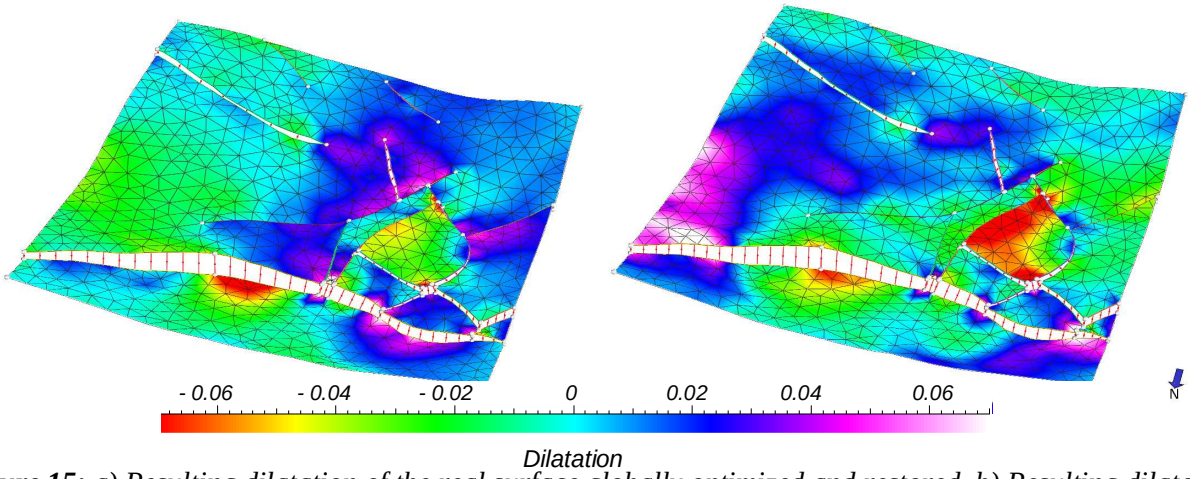

Figure 15: *a) Resulting dilatation of the real surface globally optimized and restored, b) Resulting dilatation of the same surface real simply "zipped" using the algorithm and then restored*

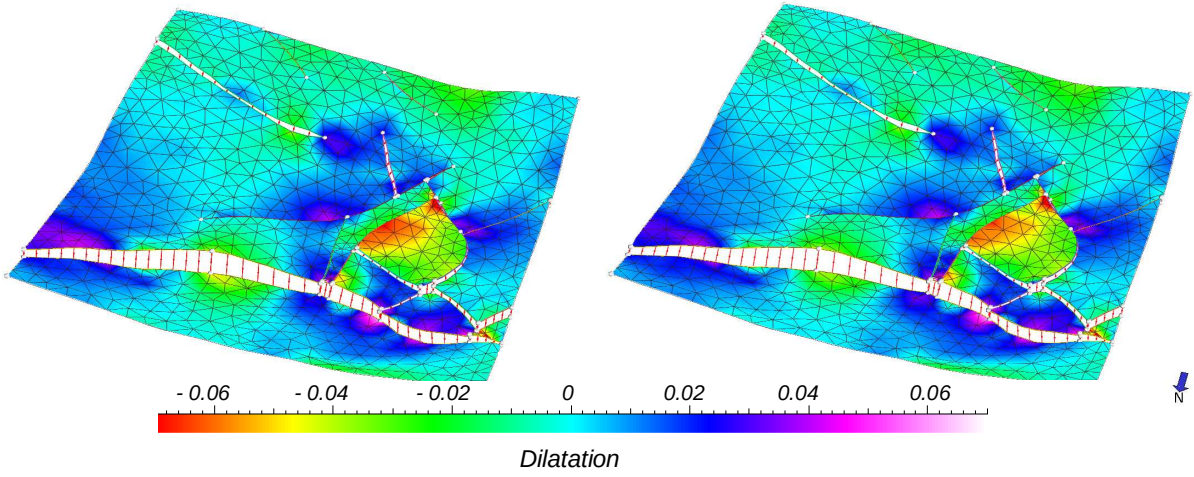

Figure 16: *Comparison between two different local optimizations*
The paths were set randomly not to bias the realizations.

References

G. Caumon and P. Muron. Surface restoration as a means to characterize transverse fault slip uncertainty, 2006. 26th Gocad Meeting, Nancy

J. Gratier, B. Guillier, and A. Delorme. Restoration and balance of a folded and faulted surface by best-fitting of finite elements: principles and applications. *Journal of Structural Geology*, 13(1):111-1115, 1991.

M. Lecour, R. Cognot, I. Duvinage, P. Thore, and J.-C. Dulac. Modeling of stochastic faults and fault networks in a structural uncertainty study. *Petroleum Geoscience*, 7:S31-S42, 2001.

L. Mace. Fast generation of 3d discrete fracture networks in respect of geology, 2005. 25th Gocad Meeting, Nancy

J.-L. Mallet. *Geomodeling*. Applied Geostatistics. Oxford University Press, New York, NY, 2002. 624 p.

J.-L. Mallet. Space-time mathematical framework for sedimentary geology. *Mathematical geology*, 36 (1):1-32, 2004

G. Massonat. Can we sample the complete geological uncertainty space in reservoir-modeling uncertainty estimates? *SPE Journal (SPE 59801)*, 5(1):46-59, 2000.

J. Massot. *Implémentation de methods de restauration équilibrée 3D*. PhD thesis, INPL, Nancy, France, 2002.

P. Muron and J.-L. Mallet. Handling faults in 3d structural restoration, 2005. 25th Gocad Meeting, Nancy.

D. Rouby, P. Cobbold, P. Szatmari, S. Demercian, D. Coelho, and J. Rici. Least-squares palinspastic restoration of regions of normal faulting - application to the Campos basin (Brazil). *Tectonophysics*, 221 :439–452, 1993.

A. Tarantola. *Inverse Problem Theory*. Elsevier, 1987. ISBN 0-444-42765-1. 630 p.

P. Thore, A. Shtuka, M. Lecour, T. Ait-Ettajer, and R. Cognot. Structural uncertainties: determination, management and applications. *Geophysics*, 67(3):840-852, 2002.